Dynamics of the baseball–bat collision

Alan M. Nathan[a)]

Department of Physics, University of Illinois at Urbana–Champaign, Urbana, Illinois 61801

A model is developed for the collision between the baseball and bat, taking into account the transverse bending vibrations of the bat. By coupling the flexible bat to the ball via a parametrized force that each mutually exerts on the other, a complete description of the collision process is obtained, including the exit speed of the ball v_f. It is shown that vibrations play an important role in determining v_f. The model is in excellent agreement with experimental data at low impact velocities. At the higher velocities more appropriate to the game of baseball, v_f is shown to coincide with the rigid-body value only over a very small region in the barrel of the bat and to drop off sharply for impacts removed from that region. Some interesting insights into the collision process are obtained, including the observation that for impacts in the barrel of the bat, the momentum transferred to the ball is essentially complete by the time the elastic wave first arrives at the handle and that any clamping action of the hands will affect the bat at the impact point only after the ball and bat have separated. This suggests that v_f is independent of the size, shape, and method of support of the bat at distances far from the impact location. © *2000 American Association of Physics Teachers.*

I. INTRODUCTION

The game of baseball has a certain fascination for physicists. In addition to the popular book by Adair,[1] there have been numerous papers in the literature[2] addressing a wide variety of issues amenable to a physics calculation. These include such diverse topics as the aerodynamics of a spinning baseball; the peculiar behavior of the knuckleball; the coefficient of restitution of a baseball and its effect on the bounce of the ball off the bat; and the dynamics of the ball–bat collision. It is this latter topic that is the subject of the present paper.

Over the years, papers in this journal have addressed both experimental and theoretical issues associated with the baseball–bat collision. Notable experimental papers are those of Brody[3] and Cross.[4] Brody studied the vibrational spectrum of a hand-held bat during and after the collision and showed that the bat behaves as a free body on the short time scale of the collision. Cross did an extensive study of the vibrational spectrum of free and hand-held bats and concluded that there exists a zone of impact locations on the barrel end of the bat where the impact forces on the hands due to recoil and vibration are minimized. Early theoretical treatments concentrated mainly on the rigid-body aspects of the collision,[5,6] but in more recent years two important theoretical papers have appeared that go beyond the rigid approximation by treating the bat as a dynamic, flexible object.

The first paper was that of Van Zandt.[7] Applying the standard theory of beams, suitably modified for a nonuniform bat, he solved the eigenvalue problem to find the normal modes for transverse bending vibrations in the bat. By coupling the ball to the bat and decomposing the motion of the bat into normal modes, he solved the collision problem taking full account of the vibrations excited in the bat and their consequent effect on the flight of the ball. In the process, he elucidated many interesting features of the collision, such as the time evolution of the motion of the bat. From the point of view of the game of baseball, the most important outcome of Van Zandt's work was the calculation of the ball exit speed, v_f, as a function of impact position along the bat. It was

shown that under typical conditions, v_f is maximized and equal to its rigid-body value when the impact is in the barrel of the bat near a node of the fundamental mode. Unfortunately, for reasons we will discuss fully herein, his calculation of v_f was flawed, resulting in a qualitatively incorrect picture of how v_f falls off as the impact point moves away from the node. One of the purposes of the present calculations is to apply a different model for the ball–bat coupling that leads to very different results for v_f.

The second paper was that of Cross,[8] who both performed experiments and did theoretical calculations of the collision of superballs with a variety of uniform aluminum beams. While his calculations do not directly address the baseball–bat collision, the calculational technique and the essential results are relevant. Particularly noteworthy is his use of a dynamic model for the coupling of the ball to the beam which corrects the shortcomings of the Van Zandt treatment. The resulting calculations of v_f are in remarkably good agreement with Cross's own data, indicating that the essential physics of the problem has been identified. Perhaps the most interesting result to emerge from those studies is that when the superball collides with an initially stationary beam, v_f is essentially independent of the length of the beam or the manner in which the ends of the beam are supported, as long as the impact location is not too close to an end. In effect, on the relatively short time scale of the collision, the ball does not ''see'' the full beam but only a segment of it that is in the vicinity of the impact point. To the extent that this result is relevant to the ball–bat collision, it provides a concise theoretical explanation of the ''free-bat'' observation of Brody.[3] Cross gives a nice interpretation of this result in the context of the interplay between collision times and pulse propagation times. We give an alternate (but completely equivalent) explanation by means of a highly simplified toy model (Appendix A) and show how this simple picture is relevant to the ball–bat collision in Sec. III.

The present paper is organized as follows. In Sec. II we develop a theoretical model for the ball–bat collision that is a hybridization of the Van Zandt and Cross techniques, uti-
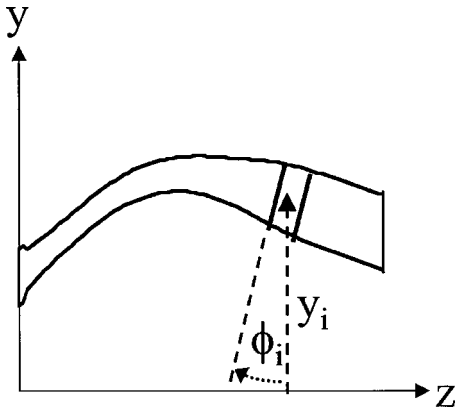
Fig. 1. Schematic (greatly exaggerated) representation of a bat that is bent and sheared. The coordinate y_i is the displacement of the ith section of the bat relative to the z axis, whereas ϕ_i is the angle between the plane of the ith section and the y axis.

lizing what we believe to be the best features of both works. Our treatment of the normal modes is identical to that of Van Zandt (Sec. II A), whereas our model for the ball and its coupling to the bat is conceptually similar to that of Cross (Secs. II B and II C). The issue of energy conservation and a discussion of the ball exit speed are addressed in Secs. II D and II E, respectively. In Sec. III we apply our model to a typical wooden bat, comparing our calculations with real data[4,9] and presenting results of practical interest to the game of baseball. We conclude with a brief summary. We relegate to Appendix B some details of the relationship between our treatment of the normal modes and that given in the textbooks.

II. MODEL FOR THE COLLISION

A. Vibrations of the bat

For this part of the calculation, we follow nearly exactly the work of Van Zandt.[7] We start with Fig. 1, where we show schematically a baseball bat that has been distorted from its equilibrium shape due to bending and shearing. The distortion of a particular segment of the bat can be characterized by its transverse displacement $y(z)$ and orientation $\phi(z)$ as a function of its coordinate z along the long axis of the bat. We divide the bat into N parallel slices of circular cross section, each of thickness Δz and each elastically coupled to its neighbors through the Young's modulus Y and the shear modulus S. Van Zandt shows in detail how to derive the equations of motion of y and ϕ for free (i.e., no external force or torque) vibrations of a bat with nonuniform cross section.[7] We have rederived and corrected slightly his equations, arriving at

$$\ddot{y}_i = \frac{S}{\rho \Delta z^2}\left[(y_{i+1}+y_{i-1}-2y_i)+\frac{A_i-A_{i-1}}{A_i}\right.$$
$$\left.\times(y_i-y_{i-1}+\Phi_{i-1})+(\Phi_i-\Phi_{i-1})\right] \qquad (1)$$

and

$$\ddot{\Phi}_i = \frac{Y}{\rho \Delta z^2}\left[(\Phi_{i+1}+\Phi_{i-1}-2\Phi_i)+\frac{I_i-I_{i-1}}{I_i}(\Phi_i-\Phi_{i-1})\right]$$
$$-\frac{S}{2\rho I_i}[A_i(y_{i+1}-y_{i-1}+\Phi_i+\Phi_{i-1})$$
$$-(A_i-A_{i-1})(y_i-y_{i-1}+\Phi_{i-1})], \qquad (2)$$

where ρ, A_i, and I_i are the density, cross-sectional area, and area moment of inertia of slice i (about an axis passing through the center of mass of the slice and normal to the $y-z$ plane), respectively, and $\Phi_i = \phi_i \Delta z$. All the bats we consider herein have a circular cross section. For solid bats (such as a typical wood bat), a slice of radius R_i has $A_i = \pi R_i^2$ and $I_i = \pi R_i^4/4$. For hollow bats (such as a typical aluminum bat), a slice of inner radius $R_{1,i}$ and outer radius $R_{2,i}$ has $A_i = \pi(R_{2,i}^2 - R_{1,i}^2)$ and $I_i = \pi(R_{2,i}^4 - R_{1,i}^4)/4$. We assume that ρ, Y, and S are uniform (i.e., independent of i), although the formalism could easily be extended to include such nonuniformities. We note that the treatment given here is equivalent to that presented in various textbooks (for example, see Graff[10]), and we show the connection in Appendix B.

We complete the statement of the problem by specifying the boundary conditions. We assume that both ends of the bat are completely free,[3] meaning that the force and torque on the end slices are due only to the next inner slices. We will show that this is a very good assumption for many purposes, including the calculation of the rebound velocity of the baseball.

In order to find the normal modes of the bat implied by our equations of motion, we assume harmonic vibrations, so that $\ddot{y}_i = -\omega^2 y_i$ and $\ddot{\Phi}_i = -\omega^2 \Phi_i$. Then Eqs. (1) and (2) can be rewritten in a compact matrix notation as

$$H\psi_n = -\omega_n^2 \psi_n, \qquad (3)$$

where

$$\psi_n \equiv \begin{pmatrix} y_{n1} \\ \vdots \\ y_{nN} \\ \Phi_{n1} \\ \vdots \\ \Phi_{nN} \end{pmatrix}$$

is a $2N$-element column matrix and H is a nonsymmetric $2N \times 2N$ matrix. One immediately recognizes this as an eigenvalue problem, requiring the diagonalization of H in order to find the normal mode frequencies ω_n and associated eigenvectors ψ_n. Standard numerical techniques are used to accomplish this, using the LAPACK subroutine package,[11] although some care is needed in applying these to a nonsymmetric matrix. We remark that the lowest two modes are zero-frequency rigid body modes corresponding to uniform translation (y_{ni} independent of i, $\Phi_{ni}=0$) and uniform rotation (y_{ni} linear in i, Φ_{ni} independent of i).

In the presence of a time-dependent external force on the ith slice, an additional term $F_i(t)/(\rho A_i \Delta z)$ appears on the right-hand-side of Eq. (1). Since the normal modes of the free vibration form a complete set, we write the solution as an expansion

$$y_i(t) = \sum_n a_n(t) y_{ni},$$

so that

$$\sum_n (\ddot{a}_n(t) + \omega_n^2 a_n(t)) y_{ni} = \frac{F_i(t)}{\rho A_i \Delta z}. \tag{4}$$

Using the orthogonality of the eigenstates,

$$\sum_i A_i y_{mi} y_{ni} \Delta z = \bar{A} \delta_{mn},$$

which defines $\bar{A}$, we project out the mth mode to arrive at

$$\ddot{a}_m(t) + \omega_m^2 a_m(t) = \frac{1}{\rho \bar{A}} \sum_i F_i(t) y_{mi}. \tag{5}$$

In the ball–bat collision, the driving force $F_i(t)$ is the force that the ball and bat mutually exert on each other. We next turn to a discussion of the ball and a model for the force.

B. Model for the ball

The baseball–bat collision is violent and involves large forces which act over a very short time and which compress the ball to a fraction of its normal size. It should be no surprise that such a collision is highly inelastic, with a significant fraction of the initial ball–bat energy dissipated into heat. The phenomenological embodiment of this inelasticity is the coefficient of restitution, which we denote by the symbol e_0. It is defined as the ratio of relative speeds after to before the collision of the ball with a perfectly rigid object:

$$\text{coefficient of restitution: } e_0 \equiv \frac{v_{\text{rel},f}}{v_{\text{rel},b}}. \tag{6}$$

With this definition, the fraction of the initial center of mass energy that is dissipated equals $1 - e_0^2$. For a baseball, e_0 is approximately 0.5, so when dropped from height h onto a massive rigid body (e.g., a hard floor), it will rebound to about $h/4$. It is clear that with such a large loss of energy, it will not be possible to understand the baseball–bat collision without accounting for the dissipation of energy in the ball.

Our approach is essentially that of Cross,[8,12] who models the ball as a nonlinear, lossy spring. For the collision of the baseball with a stationary massive rigid body, the contact force between the ball and body compresses the ball's spring, converting the kinetic energy into potential energy. At the point of maximum compression, the ball momentarily comes to rest. Then the spring expands, converting potential energy back into kinetic energy. Because the spring is lossy, not all the initial kinetic energy is restored and the ball exits with a lower speed. This process can be understood with the help of the dynamic stress–strain hysteresis curve shown in Fig. 2, in which the path taken during the compression phase is different from that taken during the expansion phase. The area bounded by the two curves is the energy dissipated

$$E_{\text{lost}} = \oint F(u) du. \tag{7}$$

Defining u as the compression of the radius of the ball, we parametrize the hysterisis curve as

$$\text{compression: } F(u) = k_1 u^\alpha,$$

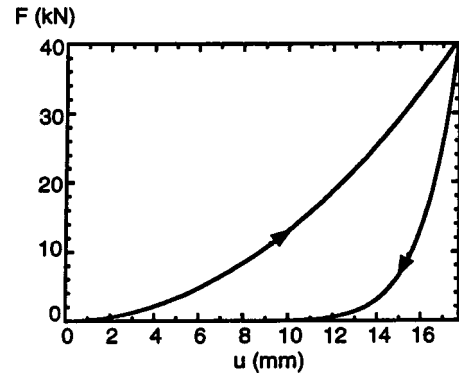$$\text{expansion: } F(u) = k_2 u^\beta, \tag{8}$$

Fig. 2. A model dynamic hysteresis curve for a typical baseball, where u is the compression of the radius of the ball and F is the force needed to achieve that compression. The curve shown is that appropriate for an impact of a 58-m/s (130-mph) ball with a rigid surface, with the coefficient of restitution $e_0 = 0.53$. The curve for the compression phase is described by $F = k_1 u^\alpha$, with $k = 6.53 \times 10^7$ and $\alpha = 1.84$.

where generally $\beta \gg \alpha$. Since the fractional energy loss is $1 - e_0^2$, Eqs. (7) and (8) lead to

$$\beta = \frac{1 + \alpha}{e_0^2} - 1.$$

The parameter k_2 is determined from the remaining parameters by equating the two expressions for the force at the point of maximum compression. Our model therefore has three parameters: the compression constant k_1, the compression exponent α, and e_0. The parameter k_1 essentially sets the overall time scale for the collision, whereas α determines the variation of the collision time with initial impact speed. For a linear spring ($\alpha = 1$) with no losses, the collision time is half of the oscillation period of the spring independent of the impact speed, whereas for $\alpha > 1$ the collision time decreases with increasing impact speed. Despite the simplicity of our model, we anticipate that the essential results of our collision calculations are not critically dependent on the details of the model, provided that the collision time and e_0 are about right. We will return to this point in Sec. II D. Since there are very few data at impact speeds relevant to the game of baseball to guide us in the choice of these parameters, we make intelligent guesses based on static hysteresis measurements[5] and dynamic measurements done at low speed[4,12,13] to arrive at the curve shown in Fig. 2, which is essentially that shown by Adair.[1] With the choice of parameters shown in the caption to Fig. 2, the collision time of our model baseball with a stationary massive rigid object, defined as the time for 99% of the impulse, is about 2.2 ms at 1 m/s, decreasing to 1 ms at 11 m/s, 0.7 ms at 45 m/s, and 0.6 ms at 67 m/s (or roughly an 85-mph fastball on a 65-mph bat), as shown in Fig. 3. Note that the collision time is not the same as the ball–bat contact time. Due to the nature of the expansion phase of the hysteresis curve, the force falls to zero while there is still considerable compression of the ball (see Fig. 2). For example, at 67 m/s the contact time is approximately 1.1 ms, whereas the collision time is 0.6 ms.

C. The ball–bat collision

We are now in a position to formulate the collision problem. We assume that the ball impacts the bat on the kth slice. The formalism could easily be generalized to allow for a
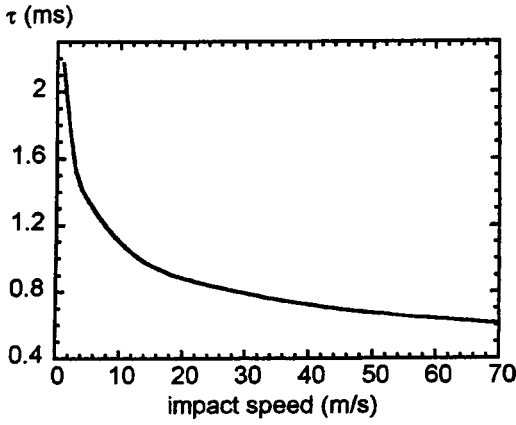
Fig. 3. Collision time τ for the impact of a baseball with a stationary massive rigid object as a function of the impact speed. These times were calculated using the parametrization of the dynamic hysteresis curve given in the caption to Fig. 2.

force spread over several slices, as was done in Van Zandt's treatment, but we have checked that the essential results of the calculation do not require that this be done. The force that the ball and bat mutually exert on each other depends on the compression of the radius of the ball according to Eq. (8). We take u to be the separation between the surface of the bat $y_k(t)$ and the center of the ball $y_{\text{ball}}(t)$ but offset by the natural radius R_{ball} so that $u=0$ corresponds to no compression. As discussed in the preceding section, the functional form of that force depends on whether the spring is compressing ($\dot{u}<0$) or expanding ($\dot{u}>0$). Putting all this together, the complete dynamics of the collision are contained in the equations

$$y_i(t) = \sum_n a_n(t) y_{ni}, \tag{9}$$

$$\ddot{a}_n(t) + \omega_n^2 a_n(t) = \frac{F(u(t)) y_{nk}}{\rho \bar{A}}, \tag{10}$$

$$m_{\text{ball}} \ddot{y}_{\text{ball}} = -F(u(t)), \tag{11}$$

$$u(t) = R_{\text{ball}} - (y_{\text{ball}}(t) - y_k(t)), \tag{12}$$

together with the normal modes, the force law, and the initial conditions. For the latter, we take $t=0$ to be the time when the ball and bat come into contact for the first time ($u=0$, $\dot{u}<0$), at which time the ball and the rigid-body modes of the bat each have initial velocities which must be specified. Under typical conditions, the ball and bat (at the impact point) are initially moving in opposite directions. Since the bat is assumed not to be vibrating prior to the collision, we set $a_n(0) = \dot{a}_n(0) = 0$ for the true vibrational modes. Standard fourth-order Runge–Kutta[14] is used to integrate the coupled differential equations numerically, using a time grid adjusted to give stable results. For a typical collision lasting less than 1 ms, a mesh of 5 μs is more than adequate. When the ball and bat separate ($u=0$, $\dot{u}>0$), the force goes to zero, the bat vibrates freely, and the ball exits with constant velocity v_f.

The technique used here is equivalent to the one used by Cross in his study of the collision of superballs with uniform aluminum beams.[8] Our implementations are different, however, since Cross works in the time domain by solving the

equations of motion directly without expanding into normal modes, whereas we work in the complementary frequency domain.

D. Energy conservation

One of the important features of our calculation is that energy conservation is respected. That is, once the ball and bat separate, the initial kinetic energy of the ball-plus-bat system is shared among the final kinetic energy of the ball, the energy contained in rigid-body modes (translation and rotation) of the bat, vibrational energy of the bat, and energy lost in the compression and expansion of the ball. This is a nontrivial feature, since it is precisely what distinguishes our calculation from that of Van Zandt, as we will discuss more fully in the following. For now, we will find it useful to develop some formulas for the partitioning of the energy of the bat among the normal modes. Following Goldsmith,[15] the energy contained in the nth vibrational mode is given by

$$E_n = \tfrac{1}{2} \rho \bar{A} (\dot{a}_n^2(\tau) + \omega_n^2 a_n^2(\tau)), \tag{13}$$

where τ is the collision time.[16] We define the force profile $\mathcal{F} \equiv F/\mathcal{I}$, where $\mathcal{I}$ is the total impulse imparted to the ball in the collision, so that

$$\int_0^\tau \mathcal{F}(t) dt = 1.$$

Assuming $a_n(0) = \dot{a}_n(0) = 0$, the solution to Eq. (10) can be written

$$a_n(\tau) = \frac{y_{nk}\mathcal{I}}{\rho \bar{A} \omega_n} \int_0^\tau \mathcal{F}(t) \sin \omega_n(\tau - t) dt,$$

from which we derive

$$E_n = \frac{\mathcal{I}^2}{2m_{\text{ball}}} R_n,$$

$$R_n \equiv \left[\frac{y_{nk}^2 m_{\text{ball}}}{\rho \bar{A}} \right] g(\omega_n), \tag{14}$$

$$g(\omega_n) \equiv \left| \int_0^\tau \mathcal{F}(t) e^{i\omega_n t} dt \right|^2.$$

These equations define R_n, which is a dimensionless parameter that is proportional to the energy transferred to the nth normal mode as a result of the collision. As we will see in the following, it plays an important role in determining the exit velocity v_f. On the other hand, the rms vibrational amplitude, velocity, and acceleration of the nth mode are proportional to $\sqrt{R_n}/\omega_n$, $\sqrt{R_n}$, and $\omega_n \sqrt{R_n}$, respectively. Therefore the vibrational amplitude and acceleration tend to emphasize more strongly the low and high frequencies, respectively, relative to the effect these frequencies have on v_f. In general, one can interpret R_n as the ratio of ball mass to an *effective* bat mass. It depends in part on the squared amplitude of the mode at the impact point (y_{nk}^2). For impact near an antinode, the term in brackets in Eq. (14) is a number of order m_{ball}/M, where M is the mass of the bat, whereas it vanishes for impact at a node. R_n also depends on the ratio of collision time to vibrational period ($\omega_n \tau$) through the response function g. Since g is the Fourier transform of $\mathcal{F}$, it
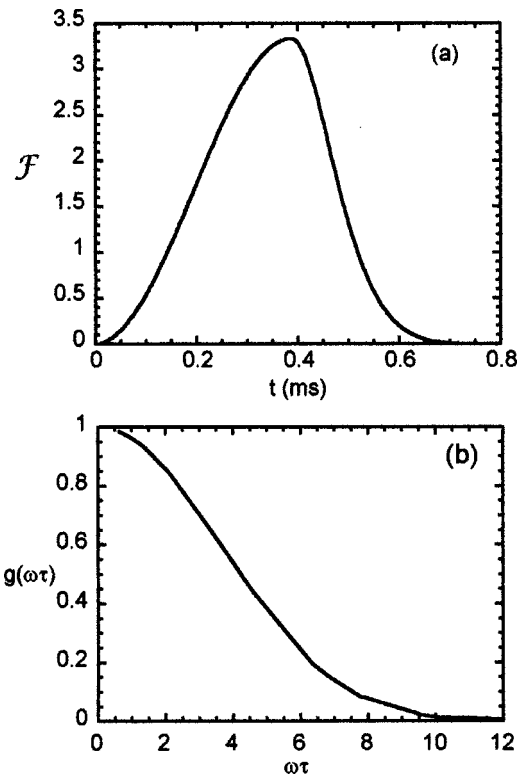
Fig. 4. (a) Force profile $\mathcal{F}(t)$ for a 70-m/s impact speed baseball on a standard wood bat, as determined from our calculations and the dynamic hysteresis curve shown in Fig. 2; (b) the curve $g(\omega)$ defined by Eq. (14) is calculated with $\mathcal{F}(t)$.

has the property that $g \to 1$ for $\omega_n \tau \ll 1$ and $g \to 0$ for $\omega_n \tau \gg 1$. Therefore normal modes with $\omega_n \gg 1/\tau$ will not be excited in the collision, in agreement with both our intuition and the toy model described in Appendix A. As an example we have solved our equations of motion for a standard wood bat (discussed in the following), using the hysteresis curve in Fig. 2 to find a typical force profile $\mathcal{F}$ [Fig. 4(a)]. For a large range of impact speeds (1–70 m/s), we find the response function g lies on a universal curve when plotted as a function of $\omega\tau$ [see Fig. 4(b)]. Moreover, because of the properties of Fourier transforms, *any* force profile having the same general shape as the one shown in Fig. 4(a) will have approximately the same response, at least for those frequencies for which g is large. Since those are the most important frequencies for determining the dynamics of the collision, this confirms the remark made earlier that the precise details of the ball–bat force are not important, as long as the time scale for the transfer of momentum is about right.[15]

E. The exit speed of the ball

One of the practical goals of our analysis is to calculate the exit speed of the ball v_f. We will find it useful to develop some formulas relating v_f to the initial speed of the ball v_{ball} and the initial speed of the bat at the impact point v_{bat}. We do this first for a rigid bat (i.e., a bat with only rigid modes but no true vibrational modes). In fact, although one need not use all the machinery we have developed to treat this case (see, for example, Brody[6]), we will find it instructive to do so. We proceed by eliminating all but the two zero-frequency rigid-body modes, which correspond to the

recoil of the center of mass of the bat and the rigid rotation of the bat about its center of mass. The calculation of R for these modes is straightforward, resulting in

$$R_0 = \frac{m_{\text{ball}}}{M}\left[1 + \left(\frac{z_k - z_{\text{CM}}}{r_\gamma}\right)^2\right], \tag{15}$$

where z_k is the location of the kth slice (the impact point) and r_γ is the radius of gyration ($I_{\text{CM}} = M r_\gamma^2$). We easily arrive at

rigid approximation: $\quad v_f = \left[\frac{e_0 - R_0}{1 + R_0}\right]v_{\text{ball}} + \left[\frac{e_0 + 1}{1 + R_0}\right]v_{\text{bat}}.$

$$\tag{16}$$

This result is expected to be valid whenever the energy contained in vibrations is small, such as when the impact point is close to one or more nodes of the lowest-frequency modes. This formula conserves momentum and angular momentum and satisfies Eq. (6); moreover the fractional energy dissipated in the ball (in the frame in which the bat is initially at rest at the impact point) is $(1 - e_0^2)/(1 + R_0)$, which is consistent with the definition of coefficient of restitution.

We attempt to generalize this result for the case in which vibrations are included. We start with the simple case in which there are vibrations in the bat but no dissipation in the ball (i.e., $e_0 = 1$). Under such conditions, one can rigorously show that the correct formula for the exit speed of the ball is given by[15]

$$e_0 = 1: \quad v_f = \left[\frac{1 - \Sigma_n R_n}{1 + \Sigma_n R_n}\right]v_{\text{ball}} + \left[\frac{2}{1 + \Sigma_n R_n}\right]v_{\text{bat}}, \tag{17}$$

where the sum is over all the normal modes (rigid and vibrational). One can easily show that this result strictly conserves energy and that the relative velocity between the ball and rigid modes of the bat is identical before and after the collision. Interpreting $\Sigma_n R_n$ as the ratio of ball mass to effective bat mass, we see that the effect of vibrations is to *decrease* the effective bat mass (in general, $\Sigma_n R_n \geq R_0$), which reduces the exit speed of the ball. Said differently, on the time scale of the collision, the bat is not a rigid body and the ball ''sees'' only a fraction of the bat mass. This is completely in accord with our intuititive understanding of the collision process, as exemplified by the toy model described in Appendix A.

One might be tempted to generalize Eq. (17) for $e_0 \leq 1$ by simply reinserting e_0 where it was in Eq. (16). Such a formula would be very appealing physically since it would clearly separate the effects of energy dissipation in the ball (which depends on e_0) and vibrational energy in the bat (which depends on the R_n). Unfortunately, although this formula is a good approximation to v_f, explicit calculation shows that it somewhat underestimates v_f by overestimating the energy dissipated in the ball. Evidently the partitioning of energy between vibrational modes in the bat and dissipation in the ball is not very straightforward. The latter energy depends directly on the maximum compression of the ball, which in turn depends on the ''give'' of the bat. When a vibrational mode is strongly excited, more of the initial impact energy is taken up in the recoil of the segment of the bat in contact with the ball, so that less energy is stored (and therefore dissipated) in the ball. This effect will be evident when we present the results of our calculations with actual bats in the next section.

The most general case can be cast in the form

$$\text{general case:} \quad v_f = \left[\frac{e_{\text{eff}} - R_0}{1 + R_0}\right] v_{\text{ball}} + \left[\frac{e_{\text{eff}} + 1}{1 + R_0}\right] v_{\text{bat}}, \quad (18)$$

which is identical to Eq. (16) if e_0 is replaced by e_{eff}. Whereas e_0 is the coefficient of restitution for the collision of the ball with a rigid surface (and therefore a property of the ball alone), e_{eff} is an effective coefficient of restitution for the collision of the ball with a flexible bat. It has the desired properties that it reduces to e_0 in the limit that vibrations are neglected and it satisfies the definition of coefficient of restitution [Eq. (6)] considering only the rigid-body motion of the bat. Moreover, the fractional energy lost in the collision to the *combined* effects of dissipation in the ball and vibrations in the bat is $(1 - e_{\text{eff}}^2)/(1 + R_0)$ in the frame in which the bat is initially at rest at the impact point. As we just discussed, there is no easy relation that allows us to separate the two forms of energy loss other than by direct numerical calculation. Moreover, Eq. (18) separates purely kinematic effects, such as the bat and ball speeds and masses, from dynamic effects that are contained completely in e_{eff}. We anticipate that e_{eff} depends strongly on the impact location but only weakly on the impact speed, as we shall see in the next section.

We finally come to the point of the different approach used by Van Zandt[7] in his treatment of the collision problem. Van Zandt attempts to improve on the rigid-body result by arguing that the relevant final relative velocity appearing in the definition of the coefficient of restitution, Eq. (6), is the difference between the ball speed v_f and the speed of the bat at the impact point, including *both* the rigid-body motion and the vibrational motion. He arrives at Eq. (16) with the important modification $R_0 \rightarrow R_0 + m_{\text{ball}} a_{\text{vib}}$, where a_{vib} is the vibrational velocity per unit impulse at the impact point at the precise time the ball and bat separate. This in turn is calculated by solving Eq. (5) with an assumed force profile $\mathcal{F}(t)$, as opposed to our technique based on solving the equations of motion directly. Unfortunately, the result has two major problems: It does not conserve energy and it does not agree with experiment. We postpone the latter problem to the next section and address here the conservation of energy problem, which can best be understood for the special case $e_0 = 1$ so that there are no losses in the ball. In that case, Eq. (17) is an exact solution that conserves energy and does not agree with the Van Zandt prescription. In Appendix A, we show via an exact toy model that the Van Zandt prescription leads to incorrect results. Based on this, we conclude that v_f is not related in any simple way to the surface speed of the bat at the moment of separation. We emphasize this point strongly not for reason of principle but because the two approaches lead to quite different results for v_f, as we shall see in Sec. III.

III. RESULTS WITH A STANDARD WOOD BAT

We have used the formalism described in the preceding sections to do a series of calculations on the bat used by Cross in his extensive set of measurements.[4] It is a 33-in./31-oz Louisville Slugger Model R161, with relevant properties listed in Table I and with a measured radius profile $R(z)$ shown in Fig. 5. Young's modulus was adjusted to reproduce approximately the measured frequency of the fundamental vibrational mode, resulting in a value ~12% larger than that

Table I. Properties of our standard wood bat including the length L, mass M, density ρ, distance of center of mass from handle z_{CM}, radius of gyration about the center of mass r_γ, Young's modulus Y, and shear modulus S.

Property	Value
L	84 cm
M	0.885 kg
ρ	649 kg/m^2
z_{CM}	0.564 m
r_γ	23 cm
Y	1.814×10^{10} N/m^2
S	1.05×10^9 N/m^2

used by Van Zandt. The calculations are not very sensitive to the precise value of the shear modulus, which was set to the same value used by Van Zandt. We set $N = 84 (\Delta z = 1 \text{ cm})$, implying that good accuracy will be achieved only for modes with wavelength large compared to 1 cm. However, as we shall see, only the lowest few modes will turn out to be important for the collision problem and for these the wavelength is ≥ 30 cm, which is safely large compared to 1 cm. We will refer to this as our "standard wood bat." We next describe the results of these calculations.

A. Normal modes

Using the input parameters discussed above, the eigenvalue problem was solved to find the normal mode frequencies $f_n = \omega_n/2\pi$ (see Table II) and eigenstates, the lowest three (nonrigid) of which are shown in Fig. 6. The lowest mode has two nodes, one approximately 17 cm (7 in.) and the other about 68 cm (27 in.) from the knob end. Each successive higher mode has one additional node. An interesting feature is that the lowest three vibrational modes have nodes in the range 68–74 cm. We will comment more on that particular feature when we discuss the ball–bat collision. Finally we note that for all of the collisions discussed below, we include vibrations up to mode 18.

B. Low-impact collision

We initially investigate low-impact collisions between ball and bat, since it will allow us to compare our results with experimental data. The data were taken on our standard wood bat by R. Cross[9] using an experimental arrangement conceptually similar to that used in his previous study of the impact of superballs on aluminum beams.[8] In the experiment a 1-m/s (2.237-mph) baseball collided with a stationary bat
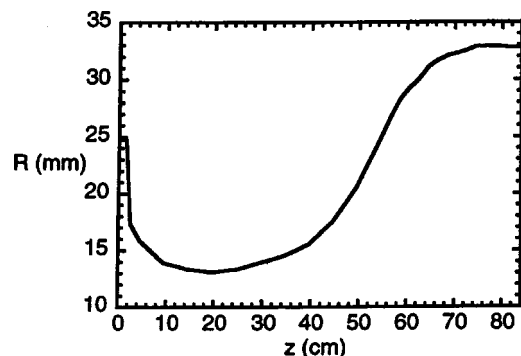
Fig. 5. Radius profile for our standard wood bat.

Table II. Lowest ten vibrational frequencies f_n for our standard wood bat calculated using the full Timoshenko theory and f'_n calculated with the approximate Euler–Bernoulli theory. Also shown are the positions of the nodes for the lowest three modes, as measured from the knob end of the bat.

Mode	f_n (Hz)	f'_n (Hz)	Nodes (cm)
1	165	169	17, 68
2	568	612	7, 39, 72
3	1177	1 334	5, 25, 50, 74
4	1851	2 220	
5	2580	3 304	
6	3359	4 637	
7	4163	6 198	
8	4972	7 962	
9	5783	9 942	
10	6598	12 139	

Fig. 7. Exit speed of a baseball in a 1-m/s impact on our standard wood bat, which is initially stationary. The solid curve is our calculated result for a flexible bat, which includes the effects of vibrations. The dotted curve is a calculation for a rigid bat. The long dashed curve (VZ) is a calculation using the technique of Van Zandt (Ref. 7). The points with error bars are the measurements of Cross (Ref. 9).

and v_f was measured as a function of impact position along the axis of the bat. The coefficient of restitution of the ball was independently measured to be $e_0 = 0.64$ for an impact at 1 m/s on a hard floor.

The data are compared with our calculation in Fig. 7, and the agreement is excellent provided e_0 is increased to 0.66, a value probably safely within the experimental uncertainty of its measurement. On the other hand, calculations for a rigid bat (i.e., a bat with only rigid-body modes but no true vibrations) follow the data only over a narrow range of impact locations, making it clear that the vibrations play a very important role in determining the exit speed of the ball. Calculations using the formalism of Van Zandt disagree strongly with the experimental results in the regions where vibrations are important. In Fig. 8(a) we examine the energy accounting. At these low-impact speeds, the collision time is quite long (~2.2 ms) so that only the lowest vibrational mode acquires any appreciable energy [Fig. 8(b)]. At the node of the lowest mode (68 cm), v_f is equal to the rigid-body value, as we would expect. However, v_f is not peaked at this location. Rather it is peaked a bit closer to the handle due to a delicate interplay between energy going into vibrations (which is minimized at the node) and energy going into rigid recoil of the bat (which is minimized at the center of mass, 56 cm). For a rigid bat, the exit velocity is peaked at precisely the center of mass. Finally we see that the energy dissipated in the ball seems to be anticorrelated with energy lost to vibrations, as we suggested in Sec. II E.
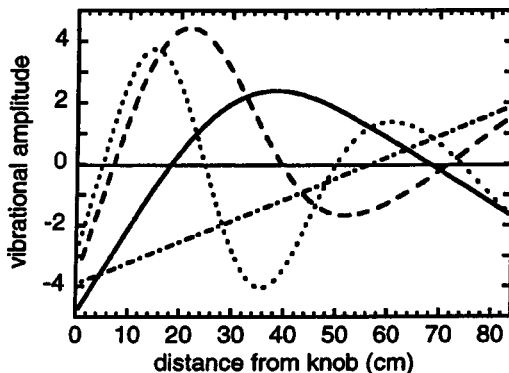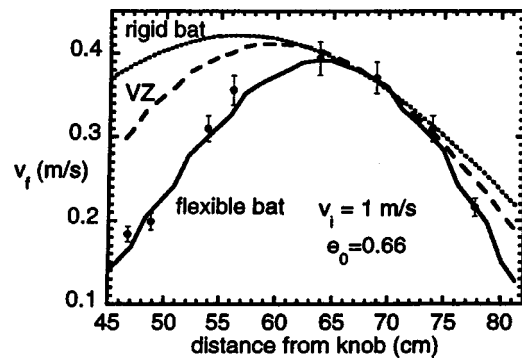
While it is gratifying that our calculations agree well with the data in Fig. 7, it should be noted that v_f does not provide a very sensitive test of the model, since only the lowest mode seems to play a role. A more sensitive test is to examine the acceleration profiles at various locations on the bat during and after the collision, since these tend to emphasize the more weakly excited high frequencies, as discussed in Sec. II D. Cross shows measurements of a variety of acceleration and velocity profiles in Figs. 2–4, 6 and 7 of his paper,[4] all of which are faithfully reproduced by our calculations. As an example we show in Fig. 9 our calculation of the data shown in Cross's Fig. 3, for which the impact point was at a barrel node of mode 2 (72 cm). The plot of the acceleration shows a clear signature for the excitation of mode 1 when viewed near a node of mode 2 (6 cm) and for the excitation of mode

Fig. 6. Eigenstates for the vibrational modes of our standard wood bat, including rigid rotation (dash–dot) and the lowest three vibrations.
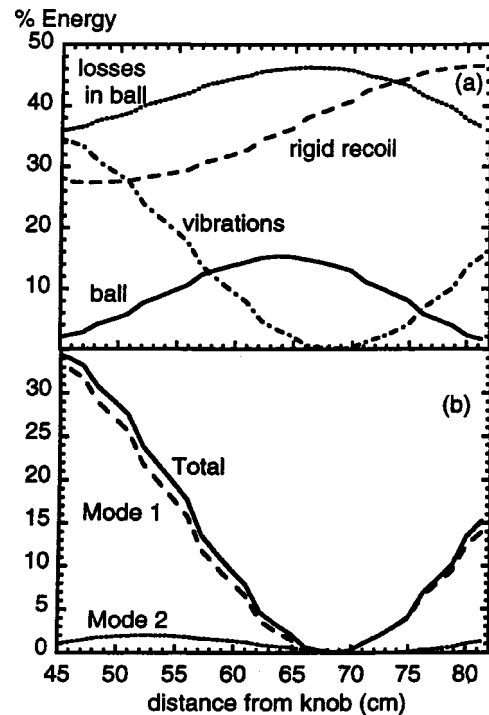

Fig. 8. The top panel shows the distribution of energy for a 1-m/s impact on our standard wood bat, initially stationary. The bottom panel shows how the vibrational energy is distributed among the normal modes.
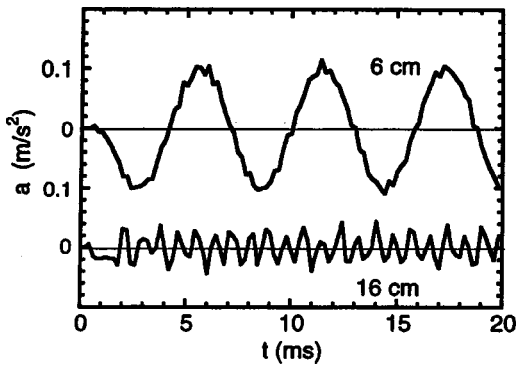
Fig. 9. Acceleration profiles for the impact of a 1-m/s baseball on our standard wood bat on the barrel at the node of vibrational mode 2. The measurement point is near a handle node of either mode 2 (6 cm) or mode 1 (16 cm). In the latter case, the effect of mode 3 is very evident, despite the fact that very little energy goes into this mode. These calculations correspond to the measurements in Fig. 3 of Cross (Ref. 4).

3 when viewed near a node of mode 1 (16 cm), despite the fact that mode 3 is essentially irrelevant in determining v_f.

This agreement between the calculations and experiment gives us confidence that our model for the bat, ball, and coupling between them is reasonable and contains all the important physics. Armed with this confidence, we next take a look at collisions with impact speeds more relevant to the game of baseball.

C. High-impact collision

We now investigate collisions with an incident ball speed of 40 m/s (90 mph), a center-of-mass bat speed of 24 m/s (54 mph), and a bat angular velocity about the center of mass of 51 s^{-1}. These numbers correspond to the bat rotating about a point 9 cm from the knob end and imply an impact speed of 71 m/s (160 mph) at a location 71 cm from the knob end (13 cm from the barrel end). We assume $e_0 = 0.50$. The results for v_f, which are shown in Fig. 10, are the primary result of this work. Additional results are shown in Fig. 11 for the energy accounting and Fig. 12 for the effective coefficient of restitution. We now turn to a discussion of these results.
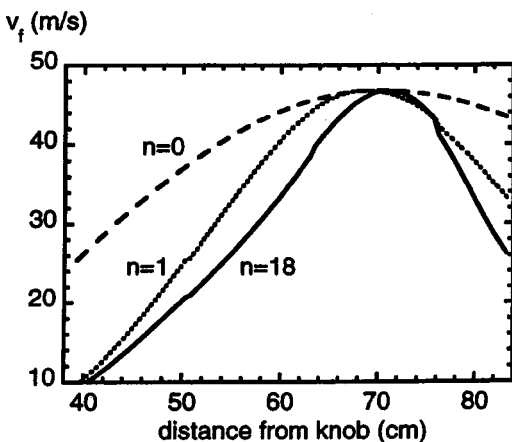

Fig. 10. Exit speed of a baseball with an initial speed of 40 m/s (90 mph) colliding with our standard wood bat, which has a CM speed of 24 m/s (54 mph) and a rotational speed about the CM of 51 s^{-1}. The three plots correspond to rigid modes only ($n=0$), rigid plus the fundamental vibration ($n=1$), and rigid plus vibrational modes up to $n=18$.
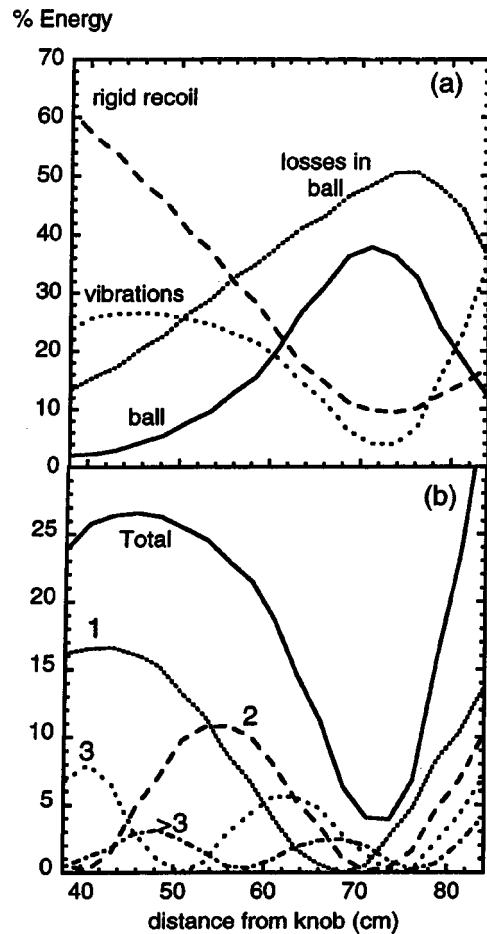

Fig. 11. The top panel shows the distribution of energy for an impact of a 90-mph ball on our standard wood bat, which has a CM speed of 54 mph and a rotational speed about the CM of 51 s^{-1}. The bottom panel shows how the vibrational energy is distributed among the normal modes.

For a rigid bat, Eqs. (15) and (16) imply that the peak of v_f lies between the center of mass (where R_0 is minimized) and the end of the bat (where v_{bat} is maximized). Interestingly, for our standard wood bat, this location nearly coincides with the location that minimizes vibrations in the bat, about 71–72 cm. Indeed, v_f is peaked there and coincides
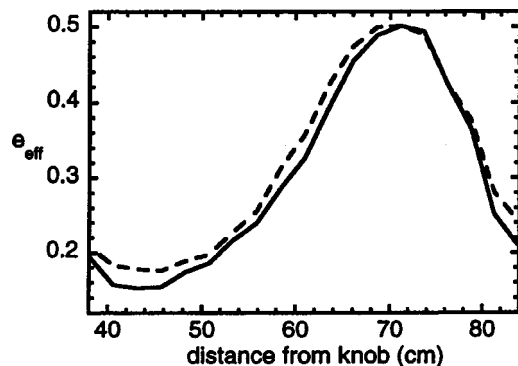

Fig. 12. Plot of e_{eff}, which is the effective coefficient of restitution for the ball–bat collision as defined by Eq. (18), for the collision described in the caption to Fig. 10 (solid line) and for a collision with half the impact speed (dashed line). For a rigid bat, e_{eff} would be 0.5, independent of impact location and impact speed.
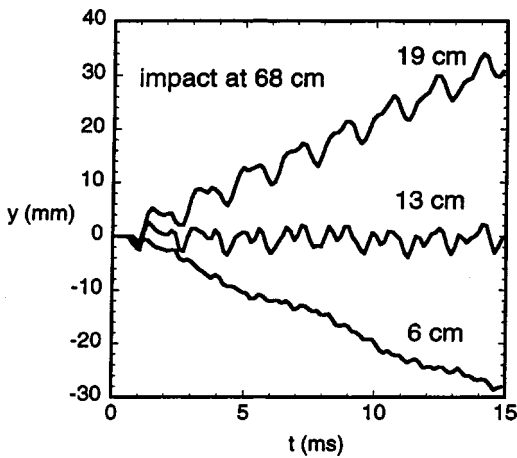
Fig. 13. Displacement (including the dc component) of three different segments in the handle of the bat with an impact location at $z = 68$ cm from the knob end, as viewed in a frame in which the segment is initially at rest.
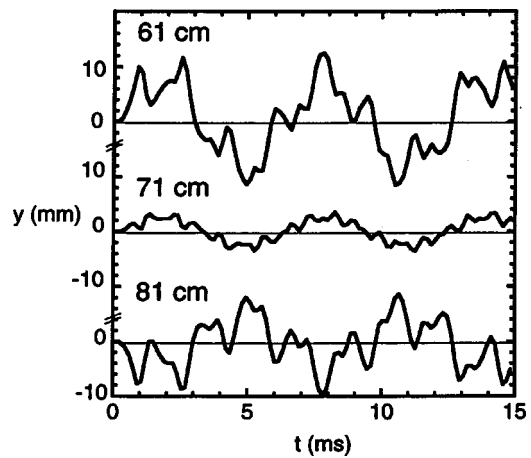

Fig. 14. Vibrational component of the displacement of a segment of the bat located 13 cm from the knob end with an impact at three different locations, as viewed in a frame in which the segment is initially at rest.

with the rigid-bat value. This location is *not* at a node of the fundamental (68 cm), as is often stated in the popular literature, but is closer to a node of mode 2 (72 cm). Actually, as remarked earlier, there are nodes of the lowest three modes in region 68–74 cm, so that the vibrational energy is not very large in this region and v_f is close to its rigid value. However, outside this region, v_f drops off rapidly. For example, at 60 cm, which is about the start of the ''fat'' part of the bat, v_f has dropped by about 25% relative to the rigid value. This is in stark contrast to the results of Van Zandt, for which the drop-off is of order 2%–3%.[7] The ball exit speed also drops off rapidly for impact locations larger than about 80 cm, which is beyond the outermost node for each of the lowest four modes. Therefore all four modes contribute to a sizable vibrational energy and a significant lowering of v_f.[17] If v_f is calculated including only the lowest vibrational mode ($n = 1$ curve in Fig. 10), the curve shifts closer to the rigid curve, which makes good sense based on energy conservation but which disagrees with Van Zandt.

The distribution of energy behaves about the way one would expect based on our previous discussion and Figs. 3 and 4. The high impact speed leads to a short collision time (typically 0.6 ms), resulting in excitation of vibrations up to about mode 4 ($f_4 = 1851$ Hz), as is evident in Fig. 11. The plots also show the anticorrelation between energy losses in the ball and the vibrational energy. In Fig. 12 we plot e_{eff} for this collision as well as for a collision at half the impact speed. The similarity confirms our earlier remark that this quantity is only weakly dependent on the impact speed. Generally, e_{eff} is slightly higher at the lower impact speed, as the longer collision time results in less effectiveness in exciting vibrations.

It is interesting to investigate the motion of the handle resulting from the impact. In Fig. 13 we show the displacement of three segments in the handle of the bat (in a frame of reference in which the segments are initially at rest) when the ball impacts at $z = 68$ cm. Several interesting features are apparent. There is both a dc component due to the rigid-body modes and an oscillating component due to the true vibrations. The measurement point at 13 cm is the center-of-percussion[6] conjugate to the impact point, so the dc component vanishes. For the measurement points at 6 and 19

cm, which are on opposite sides of the center of percussion, the bat recoils in opposite directions, with the 6-cm point moving in the direction of the rebounding ball. The vibrations are dominated by the second and third modes, since the impact point is close to a node of the primary. For the measurement point at 6 cm, the vibrational amplitude is considerably weaker since this point is very close to nodes of both the second and third modes (see Fig. 6). The vibrational amplitude and waveform observed in the handle depend on the impact location. This is shown in Fig. 14 for three different impact locations ($z = 61$, 71, and 81 cm) and for a measurement point at 13 cm, where the dc component has been removed in order to emphasize the vibrational components. The vibrational amplitude in the handle is minimized at the 71-cm impact point, as one might expect based on consideration of the vibrational energy (Fig. 11). There is a wealth of interesting information about the vibrational spectrum contained in these waveforms, but we will not comment further on that.

Perhaps the most interesting feature of Fig. 13 is that the handle of the bat responds to the impact only after a measurable delay. We investigate this point on a finer time scale in Fig. 15, where we show the velocity of the bat (including the dc component) at the 13-cm point due to an impact at $z = 68$ cm. It is evident that the handle does not start to respond until about 0.5–0.6 ms after the initial contact, at which time the transfer of momentum to the ball is nearly complete. Any clamping action of the hands will not affect the bat at the impact location until one round trip, or about 1.0–1.2 ms, by which time the ball and bat have just started to separate (see the discussion in Sec. II B). This justifies the treatment of the bat as a free object on the time scale of the collision. The hands undoubtedly do affect the vibrations of the bat,[4] but only after the collision is complete. It is interesting to see whether the propagation time of the velocity pulse is consistent with the expected group velocity of elastic waves in the bat. Guided by Fig. 4 and using a collision time of 0.6 ms, we estimate that the frequency spectrum of elastic waves is peaked at zero frequency and has a spread Δf of about 1600 Hz. Taking the average separation between nodes as half a wavelength, we find the corresponding spread of inverse wavelengths $\Delta(1/\lambda)$ to be about 2.25 m^{-1}. Therefore the group velocity $v_g \sim \Delta f / \Delta(1/\lambda)$ is about 700 m/s. This
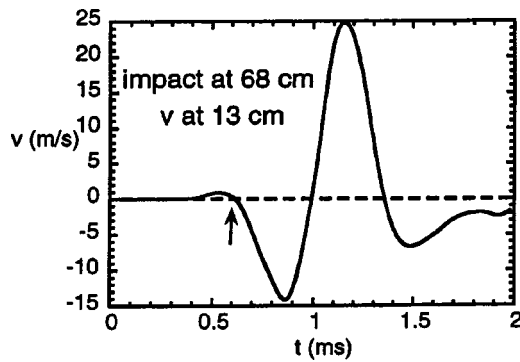
Fig. 15. Velocity of a segment of the bat 13 cm from the knob end with an impact at 68 cm, as viewed in a frame in which the bat is initially at rest. The arrow indicates the time at which 99% of the impulse to the ball has occurred. This plot shows that the handle has barely started to react by the time the collision is complete.

would imply a propagation time from 68 to 13 cm of about 0.8 ms, which is roughly consistent with Fig. 15. Because the phase velocity of the elastic waves is a strong function of frequency, there is considerable dispersion in the pulse, with the higher frequency components arriving first.

We can carry this analysis further by considering the collision of a ball with a bat that is pivoted about a point on the handle. This is exactly the condition under which bats are certified for use by the NCAA under their new standards,[18] so it is both an interesting and a practical question as to whether a pivoted bat behaves differently than a free bat (which we have shown is equivalent to a hand-held bat as far as the ball is concerned). Treatment of a pivoted bat requires modifying our equations of motion by adding an additional force at the pivot point that is adjusted at each step in the numerical integration to make the acceleration of the bat at that point vanish. We compare a pivoted to a free bat in Fig. 16, where we have assumed in both cases a 40-m/s incident ball on a bat that is rotated about a pivot point located 15 cm from the knob end with an angular velocity of 56 s^{-1}. Over the range of impact locations shown, the calculated v_f is remarkably identical in the two cases, despite the fact that the results are very different if we treat the bat as a rigid body. This result makes sense when analyzed in the context of pulse propagation times. For an impact at 50 cm, we estimate that the time for the elastic pulse to make the round trip to the pivot and back is approximately 1 ms, which is longer than the collision time of 0.6 ms and a little shorter
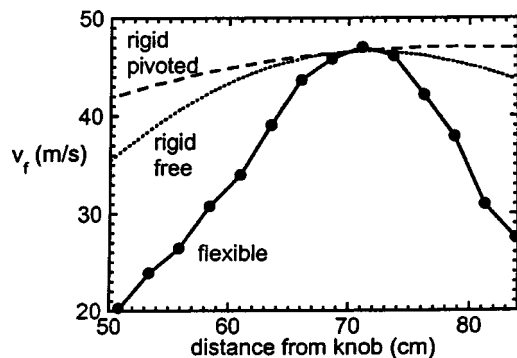

Fig. 16. Calculations comparing the exit velocity of the ball for a free (full curve) and pivoted (points) bat. The dotted and dashed curves are calculations for a rigid free and pivoted bat, respectively.
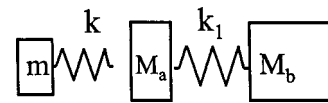

Fig. 17. Toy model for the ball–bat collision.

than the contact time of 1.2 ms. For impact locations closer to the handle than 50 cm, the analysis of the results is complicated by the fact that multiple collisions occur due to the low exit speed of the ball and the large vibrational amplitude in the bat.

One can similarly investigate the effect of modifying the bat by changing either the length or the diameter of the handle. Not surprisingly, we find that for impacts far from the handle (e.g., in the barrel region), v_f is insensitive to the detailed size and shape of the handle or to the means by which it is suspended (e.g., free, pivoted, or clamped). As in our toy model, the ball doesn't know that the far end of the bat is there. This conclusion is completely in accord with the measurements, calculations, and analysis of Cross for the collision of superballs with aluminum beams.[8]

IV. SUMMARY

We have developed a model for the collision between the baseball and bat that takes into account the vibrational degrees of freedom of the bat. Although our technique for finding the normal modes closely parallels that of a previous investigation, our technique for the coupling between the ball and bat differs sharply. We have shown the model to be in excellent agreement with experimental data at low impact velocities. At the higher velocities more appropriate to the game of baseball, we show that the vibrations excited in the bat play a crucial role in determining the ball exit speed v_f. In particular v_f coincides with the rigid-body value only over a very small region in the barrel of the bat and drops off sharply for impacts removed from that region. Our calculations give several insights into the collision process. The most interesting of these is the observation that the handle of the bat has barely started to react to the impulse by the time the momentum transferred to the ball is complete and that any clamping action of the hands will affect the bat at the impact point only after the ball and bat have separated. From this we have concluded that the exit speed of the ball is essentially independent of the detailed size, shape, and method of support of the bat at distances far removed from the impact location.

ACKNOWLEDGMENTS

APPENDIX A: A TOY MODEL

We propose the toy model shown in Fig. 17 as a way to understand the essential features of the ball–bat collision. We model the ball as a massless linear spring of force constant k with a block of mass m attached to one end and the
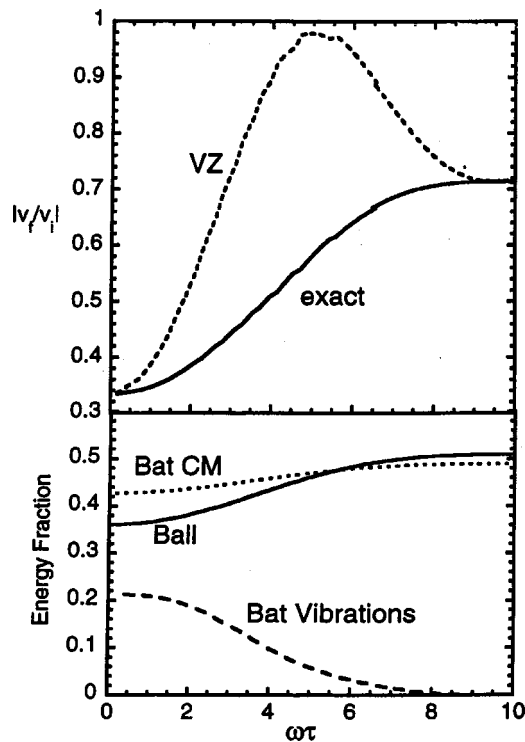
Fig. 18. Results of the toy model calculation of v_f/v_i (top panel) and the energy partitioning (bottom). In the top panel, the solid curve is the result of our exact calculation whereas the dashed curve (*VZ*) is that calculated using the prescription of Van Zandt (Ref. 7). In the bottom panel the solid, dotted, and dashed curves are, respectively, the energy fractions going into the ball, the center-of-mass motion of the bat, and the vibrations of the bat.

other end free. We model the bat as two masses M_a and M_b connected by a linear spring of force constant k_1. This is a one-dimensional problem, with the ''bat'' initially at rest and the ball initially with speed v_i. The toy bat has exactly two degrees of freedom, corresponding to the center-of-mass motion and to the excitation of the spring. The ball impacts the mass M_a and the goal is to find the rebound speed of the ball and the energy going into recoil and vibrations of the bat after the ball and bat separate. This is a problem that can be solved analytically, although we will find it more convenient to do it numerically.

Given the masses and v_i, the essential parameter that determines v_f is $\omega\tau$, where $\omega = \sqrt{k_1/\mu_{ab}}$, μ_{ab} is the reduced mass of the bat, and τ is the collision time (approximately $1/2$ the period of oscillation of the ball spring). For definiteness, we fix m, M_a, and M_b to be 1, 2, and 4 units, respectively, set $k=1$, and calculate v_f as a function of $\omega\tau$ (varying k_1). Our results are shown in Fig. 18. In the two extreme regimes, $\omega\tau \gg 1$ and $\omega\tau \ll 1$, a simple physical interpretation is possible. For $\omega\tau \gg 1$, corresponding to a very stiff bat spring, the ball pushes slowly on the bat, which recoils as a whole without exciting the spring. This is just elastic scattering of a mass 1 object from a mass 6 object, from which we easily calculate $v_f/v_i = 0.714$. On the slow time scale of the collision, the bat is completely rigid and all the energy is shared between the ball and the center-of-mass mode of the bat. The opposite extreme, $\omega\tau \ll 1$, corresponds to a very loose bat spring. On the comparatively short time scale of the collision, M_a is essentially uncoupled from M_b, so that kinematically the collision looks like elastic scattering of a mass 1 object from a mass 2 object. In effect, the ball does not ''know'' that M_b is there. We easily find $v_f/v_i = 0.333$, with a substantial amount of the energy going into the vibrational mode of the bat. Also shown is v_f/v_i predicted from the prescription of Van Zandt,[7] which disagrees with the exact calculation except in the two extreme limits. A detailed look at the calculations shows that the exit speed of the ball is not related in a simple way to the speed of M_a at the time of separation.

The essential features of this toy model are applicable in diverse areas of physics. For example, in the scattering of electrons from a composite system such as a nucleus, the electron can scatter elastically from the total charge distribution in the nucleus (a process simply called elastic scattering) or can scatter from individual protons in the nucleus (commonly called quasielastic scattering). Whenever the energy of the electron is low compared to typical binding energies in the system (equivalent to long time scales in our classical problem), only elastic scattering is possible. At higher energies (or equivalently short time scales), quasielastic scattering dominates.

APPENDIX B: EQUATIONS OF MOTION IN THE CONTINUUM LIMIT

In this Appendix, we show the connection between our equations of motion and those of Graff.[10] We take the continuum limit ($N \to \infty$, $\Delta z \to 0$) of Eqs. (1) and (2), arriving at the so-called Timoshenko equations for the free vibration of a nonuniform beam:

$$\rho A \ddot{y} = \frac{\partial V}{\partial z} \tag{19}$$

and

$$\rho I \ddot{\phi} = \frac{\partial M}{\partial z} - V, \tag{20}$$

where the shearing force V is given by

$$V = SA\left(\frac{\partial y}{\partial z} + \phi\right) \tag{21}$$

and the bending torque M given by

$$M = YI \frac{\partial \phi}{\partial z}. \tag{22}$$

In fact, these equations are even more general than our original ones, since they are valid even if Y, S, and ρ are nonuniform. Indeed, we could have used these as our starting point. One often combines these coupled second-order (in time) differential equations into the following single fourth-order equation, which we have generalized here for nonuniform cross section:

$$\rho A \ddot{y} = -\frac{\partial^2}{\partial z^2}\left(YI \frac{\partial^2 y}{\partial z^2}\right) + \rho\left(1 + \frac{Y}{S}\right)\frac{\partial^2(I\ddot{y})}{\partial z^2} - \frac{\rho^2 I}{S} \ddddot{y}. \tag{23}$$

A common approximate treatment is effected by neglecting both the deformation due to the shear forces ($S \to \infty$, $\partial y/\partial z \to -\phi$, with V finite) and the moment of inertia in Eq. (20) (so that $\partial M/\partial z = V$). In Eq. (23) this is equivalent to neglecting the last two terms on the right-hand-side, leading to the much simpler Euler–Bernoulli equation:[10]

$$\rho A \ddot{y} = -\frac{\partial^2}{\partial z^2}\left(YI\frac{\partial^2 y}{\partial z^2}\right). \tag{24}$$

From the structure of Eq. (23), it is easy to see that the neglect of the moment of inertia and shear strain introduces errors into the vibrational frequencies of order $(R/\lambda)^2$ and $(Y/S)(R/\lambda)^4$, respectively, where R is a characteristic radius of the bat and λ is the wavelength of the vibration. If one were so inclined, one could use the solutions of Eq. (24) as a starting point and treat the neglected terms in perturbation theory. A comparison between the Timoshenko and Euler–Bernoulli theories for the lowest ten vibrational frequencies is given in Table II for our standard wood bat. One sees that the full theory lowers the frequencies by an amount that increases dramatically for the higher modes. Cross used the Euler–Bernoulli theory in his study of the collision of super-balls with aluminum beams.[8] In the present work, we exclusively use the full Timoshenko theory.

[a])Electronic mail: a-nathan@uiuc.edu

[1]Robert K. Adair, *The Physics of Baseball* (HarperCollins, New York, 1994), 2nd ed., pp. 71–79.

[2]A useful compendium of articles, mostly reprinted from the *American Journal of Physics*, are contained in the book edited by Angelo Armenti, Jr., *The Physics of Sports* (American Institute of Physics, New York, 1992). Besides the reprinted articles, there is an extensive bibliography with references to many additional articles.

[3]H. Brody, ''Models of baseball bats,'' Am. J. Phys. **58**, 756–758 (1990).

[4]R. Cross, ''The sweet spot of a baseball bat,'' Am. J. Phys. **66**, 772–779 (1998).

[5]P. Kilpatrick, ''Batting the ball,'' Am. J. Phys. **31**, 606–613 (1963).

[6]H. Brody, ''The sweet spot of a baseball bat,'' Am. J. Phys. **54**, 640–643 (1986).

[7]L. L. Van Zandt, ''The dynamical theory of the baseball bat,'' Am. J. Phys. **60**, 172–181 (1992).

[8]R. Cross, ''Impact of a ball with a bat or racket,'' Am. J. Phys. **67**, 692–702 (1999).

[9]R. Cross (private communication).

[10]K. F. Graff, *Wave Motion in Elastic Solids* (Oxford U.P., Oxford, 1975), pp. 140–212.

[11]The Linear Algebra Package (LAPACK) subroutines are downloadable from the WWW site http://nacphys.phys.orst.edu/lapack.

[12]R. Cross, ''The bounce of a ball,'' Am. J. Phys. **67**, 222–227 (1999).

[13]The rules of Major League Baseball specify that e_0 for a baseball lies in the range 0.514–0.578 for a 26 m/s hitting a massive stationary object. There is much debate as to the actual e_0 for more realistic impact speeds of 70 m/s and whether the baseballs of today have a larger e_0 at these speeds than did the baseballs of yesteryear.

[14]W. H. Press *et al.*, *Numerical Recipes* (Cambridge U.P., Cambridge, 1986), p. 553.

[15]W. Goldsmith, *Impact* (Arnold, London, 1960), pp. 108–129.

[16]This expression ignores the vibrational energy associated with the shearing motion as well as the rotational energy of the individual slices. As discussed in Appendix B, these effects are expected to be small. Indeed, we have verified by direct calculation that less than 1% of the energy appears in these modes under conditions typical for the ball–bat collision.

[17]A more realistic model for the ball would allow for a coefficient of restitution e_0 which decreases slowly with increasing impact speed, as discussed by Adair in his book (Ref. 1). Since the impact speed for a bat rotated about its handle depends on impact position, this would imply an e_0 that decreases with increasing distance from the knob. For the high-impact collision described in the text, e_0 is estimated to vary by approximately 15% for impacts between 40 and 80 cm. Explicit calculation shows that this would change the quantitative (but not the qualitative) features of v_f in Fig. 10, making it slightly broader on the low side of the peak at 71–72 cm. For example, relative to the peak, v_f at 40 cm would be boosted by only about 10%.

[18]The September 1999 report that establishes procedures for certification of bats can be found on the WWW at the site http://www.ncaa.org/releases/makepage.cgi/miscellaneous/1999092901ms.htm.